Published in: Nuclear Medicine & Biology (2005), vol.32, iss.5, pp.431-436
Status: Postprint (Author's version)

In vitro and in vivo evaluation of [^{123}I]-VEGF$_{165}$ as a potential tumor marker

Bart Cornelissen[a], Ruth Oltenfreiter[a], Veerle Kersemans[a], Ludovicus Staelens[a], Francis Frankenne[b], Jean-Michel Foidart[b], Guido Slegers[a]

[a]*Laboratory for Radiopharmacy, Ghent University, B-9000 Gent, Belgium*
[b]*Laboratory of Tumour and Developmental Biology, University of Liège, Sart-Tilman, B-4000 Liège, Belgium*

Abstract: One of the research challenges in oncology is to develop new biochemical methods for noninvasive tumor therapy evaluation to determine whether the chemotherapeutics is effective. Vascular endothelial growth factor (VEGF) was labeled with radioiodine and evaluated in vitro as well as in vivo, using A2058, a melanoma cell line overexpressing VEGFR-1 and -2. Saturation binding analysis with [^{125}I]-VEGF resulted in a K_d of 0.1 nM. Internalization assays indicate the preserved ligand induced internalization and metabolization of the tracer. Biodistribution studies with [^{123}I]-VEGF in wild type and A2058 tumor-bearing athymic mice showed low background activity and a tumor to reference tissue ratio of maximum 6.12. These results suggest that [^{123}I]-VEGF is a potentially suitable tracer for tumor therapy evaluation.

Keywords: Cancer; Vascular endothelial growth factor; Molecular imaging receptor scintigraphy

1. Introduction

Angiogenesis plays an essential role in embryogenesis, normal tissue growth, wound healing and the female reproductive cycle. It also plays a major role in various diseases. Special interest is focused on tumor growth, since tumors cannot grow more than a few millimeters in size without developing a new blood supply.

Among others, vascular endothelial growth factor (VEGF-A) is one of the key molecules for angiogenesis and for the survival of the endothelium. It is a specific endothelial cell mitogen and a strong vascular permeability factor. VEGF-A is a heparin-binding glycoprotein, secreted as a homodimer of 45 kDa by many different cell types. Several variants of VEGF-A have been described, but VEGF$_{165}$ is the most predominant protein. VEGF-A transcription is highly activated by hypoxia and by oncogenes like H-*ras* and several transmembrane tyrosine kinases, such as epidermal growth factor receptor and erbB2. Together, these pathways account for a significant up-regulation of VEGF-A in tumors compared to normal tissues and are of prognostic importance [1,12]. VEGF signaling is mediated mainly by two receptors: VEGFR-1 (K_d= 10-20 pM for VEGF$_{165}$) and VEGFR-2 (K_d=75-125 pM for VEGF$_{165}$). The affinity for the VEGFR-1 is higher, but the cellular response is mainly dominated by VEGFR-2 [2].

One of the research challenges in oncology is to develop new biochemical methods for tumor therapy evaluation to determine whether the chemotherapeutics is effective [3,4]. This article presents the evaluation of the [$^{123/125}$I]-VEGF$_{165}$ for future use as a radiodiagnostic to evaluate the effect of farnesyl transferase inhibitors in tumor-inoculated athymic mouse models. Although [^{123}I]-VEGF$_{165}$ and [^{123}I]-VEGF$_{121}$ have been used before in vitro as well as in patients by Li et al. [5,6], biodistribution studies in animals, which are of prior importance, are not reported. Li also showed that the labeled VEGF$_{165}$ isoform showed affinity to more cell lines than the VEGF$_{121}$ and is therefore preferred in this study.

The synthesis, in vitro evaluation of and biodistribution of [^{123}I]-VEGF$_{165}$ in wild-type NMRI mice as well as in tumor-bearing athymic mice are reported and discussed. If the parameters of the radiopharmacon, mainly kinetics and tumor uptake ratios, are sufficient, in vivo therapy evaluation is considered for chemotherapeutics that interfere with the VEGFR pathway, such as tyrosine kinase inhibitors or farnesyl transferase inhibitors [1].

2. Materials and methods

2.1. Synthesis of [^{123}I]-VEGF and [^{125}I]-VEGF

Synthesis of both radioligands was performed in similar conditions, using the Iodogen technique. Iodogen (1,3,4,6-tetrachloro-3α,6α-diphenylglycouracil, Pierce, Aalst, Belgium) was coated to polypropylene vials using 70 μg of Iodogen per 200 μl of chloroform per vial (Aldrich, Bornem, Belgium). After evaporation of the solvent under N_2-atmosphere at room temperature, the vials were stored at 4°C. Two micrograms of VEGF (Peprotech,

London, UK) and the required amount of carrier- free $Na^{123}I$ or $Na^{125}I$ (Bristol-Meyers Squibb, Brussels, Belgium) was added to a Iodogen-coated vial. Total reaction volume was adjusted to 140 µl, using a 0.1 M potassium phosphate buffer at pH 8.5. After 10 min at room temperature the mixture was removed from the Iodogen vial to stop the reaction. Bovine serum albumin (BSA) solution was added (Sigma, Bornem, Belgium; 250 mg BSA per 100 ml 0.1 M phosphate-buffered saline [PBS] at pH 7.2, referred to as PBS/BSA). VEGF tracer and remaining radio-iodide were separated using a standard prepacked PD-10 SEC column (Size Exclusion Chromatography, Amersham Pharmacia Biotech, Uppsala, Sweden) using PBS/BSA as eluent [7].

The adsorption of the tracer to the preparative SEC column was checked using an already purified [^{123}I]-$VEGF_{165}$ solution in PBS/BSA. From this adsorption value and the initial mass of protein used, the molar fraction eluted from the column was calculated. Specific activity was calculated as the amount of radioactivity per microgram of $VEGF_{165}$ recovered at end of purification. Quality control was performed using SEC-HPLC and the radiochemical purity was calculated. Stability of the tracer was assessed in both PBS and DMEM growth medium (Bio-Whittaker, Verviers, Belgium) after various times of incubation, using PD-10 separation.

2.2. Cell cultures and binding assay

A2058 (human melanoma) cells were cultured in DMEM (Gibco, Paisley, UK), enriched with 10% of fetal bovine serum (FBS, Gibco), supplemented with 1% penicillin-streptomycin mixture (Bio-Whittaker) and 1% L-glutamine (Bio-Whittaker). Split ratios were 1:20 weekly. Both cell lines grew in an anchorage-dependent manner in tissue culture flasks and Falcon 12-well tissue culture plates (Novolab, Belgium).

Saturation binding analysis was performed on A2058 cells in 12-well cell culture plates, using three wells for each data point. After stripping of all receptor-bound proteins, using 0.1 M glycine-HCl buffer (pH 3), basic medium without FBS and increasing amounts of [^{125}I]-$VEGF_{165}$ radiotracer were added to the cells. The total incubation volume was adjusted to 1 ml. The cells were incubated for a period of 2 h at 4°C to avoid internalization. After 2 h, the supernatant was removed and the cells were washed with 1 ml of cold PBS (4°C). The supernatant and washing buffer were pooled and counted for radioactivity ("free ligand") with an automated NaI(Tl) gamma counter (CobraII Series, Canberra Packard, Meriden, CT). Two hundred microliters of trypsin-EDTA was added to the cells and incubated at 37°C for 10 min. After addition of 1800 µl of PBS, the suspension was removed and counted for radioactivity ("bound"). This experiment was repeated three times. Saturation plots were calculated using the Prism Graph Pad software (Graphpad Software), resulting in best fits for K_d, B_{max} and nonspecific binding coefficient [8]. Results were normalized for cell count, which was obtained from parallel cell culture plates, using the trypan blue method. Also, a displacement experiment with unlabeled VEGF was carried out on A2058 cells, as described by Li et al. to examine the specificity of the binding of the tracer.

In order to investigate tracer internalization, A2058 cells, grown in 12-well tissue culture plates, using three wells per data point, were incubated at 37°C for various times (ranging from 20 min to 3 h) in the presence of 0.7 nM [^{125}I]-$VEGF_{165}$. After incubation, the supernatant was removed; cells were washed with basic medium and treated with 0.1 M glycine-HCl buffer (pH 2.5) for 6 min at 4°C to remove surface-bound ligand. Cells were detached using 200 µl NaOH solution (1 M, incubation for 30 min at 37°C), re-suspended with 800 µl of water, removed and counted for radioactivity [4,9]. This experiment was repeated three times.

2.3. Biodistribution of [^{123}I]-$VEGF_{165}$

Both male white NMRI mice (20-25 g) and male Swiss *nu/nu* mice (nude, 20-25 g) were purchased from Bio-services (Schaijk, The Netherlands). All animals were treated according to the regulations of the Belgian law and animal experiments were approved by the local ethical committee. All manipulations with Swiss *nu/nu* mice were carried out in sterile conditions.

Biodistribution on tumor-bearing mice was carried out using A2058 tumors. Cells were harvested by trypsinization or using a cell scraper in growth medium. After centrifugation for 5 min at 100 x*g*, cells were resuspended in serum-free growth medium. Cells were counted using the trypan blue method. Male Swiss *nu/nu* athymic mice were injected subcutaneously in the right flank with a suspension of approximately $5x10^6$ A2058 cells in a total volume of 200 µl serum-free growth medium. Tumor growth curves were obtained using daily sliding caliper measurement. Tumor volume was calculated as $V=0.4\ a^2b$, a and b being the short-axis and the long-axis of the tumor, respectively. Tumor-bearing mice were used in the biodistribution studies when tumor volume was approximately 1 ml.

NMRI and tumor-bearing nude mice were both injected intravenously through the lateral tail vein with a 100 µl solution of 2 µCi of [^{123}I]-VEGF$_{165}$ (4 µCi per 100 µl for all intervals longer than 2 h). At various time points (20 s to 48 h for NMRI mice and 1 to 6 h for tumor-bearing nude mice) postinjection (p.i.), the animals were sacrificed by decapitation and blood was recovered (n =3 per time point). All organs (lung, liver, stomach, spleen, bladder, large and small intestines, mesenterium, brain, skin, muscle, tail and heart) were removed, briefly washed in physiological saline to remove blood, dried, weighed and counted for radioactivity using an automated NaI(Tl) gamma counter (CobraII Series). In case of tumor-bearing mice, also the left thigh muscle (reference tissue) and the tumor were dissected and treated as mentioned above. Blood was weighed and counted like the organs. The injected activity was calculated by weighing the syringes before and after injection and by the use of a dilution series of the injected tracer solution, which is also weighed and counted for radioactivity using the same CobraII gamma counter. The concentration of radioactivity in the organs was expressed as percentage of the injected dose per gram of tissue (%ID/g). Excretion was recovered and counted for radioactivity and expressed as %ID [7,9]. Results for tumor uptake were expressed as a ratio %ID/g tumor vs. left thigh muscle as a reference organ.

2.4. In vivo imaging

Dynamic gamma camera imaging was performed in NMRI mice using a Toshiba GCA-9300 A/hg SPECT camera in the planar mode equipped with a high-resolution parallel-hole collimator. All images were acquired into 128x128 matrices (FOV: 23.5x12.46 cm) and with a photopeak window set at 15% around 159 keV. At the same time a syringe with a known amount of radioactivity was scanned to allow the semiquantification of the results of the ROI analysis. The animals were anesthetized intraperitoneally with 75 µl (1.5 mg) of a pentobarbital solution (Nembutal, 20 mg/ml, Ceva Santé Animale, Belgium) before starting the imaging experiments. After sedation, 3.7 MBq of [^{123}I]-VEGF$_{165}$ was injected via the lateral tail vein. Eighty images of 1 min each were taken. ROIs were drawn using a MRI maximum intensity projection [10].

Fig. 1: *Representative chromatogram of the preparative purification of [^{123}I]-VEGF$_{165}$ with a PD-10 column. The first peak at fractions 7-10 reflects the elution of the labeled compound. The second peak at fractions 18-20 reflects the elution of the remaining free iodine isotope.*

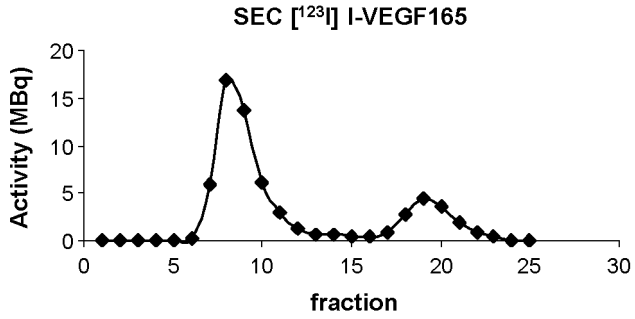

Table 1: *Stability of [^{125}I]-VEGF at 4 and 24 h after start of incubation at 20°C or 37°C in PBS or DMEM*

Temperature	**PBS**		**DMEM**	
(°C)	4 h (%)	24 h (%)	4 h (%)	24 h (%)
20	97	77	96	70
37	87	-	-	-

The stability is expressed as the percentage of intact native labeled peptide (n =3, standard deviations were < 1%).

In order to exclude that increased vascularization is the cause of the tumor to muscle ratio of 6.12 (±2.11), a ^{99m}Tc-HSA (human serum albumin) planar scintigraphy scan was performed to look at blood flow. Animals (n=5) were sedated as described above and injected with 3.7 MBq of ^{99m}Tc-HSA. One static image was taken from 5 to 10 min p.i. Also, a displacement study was performed using 80 µg of VEGF$_{165}$, co-injected with the tracer. Six animals bearing an A2058 tumor were scanned with [^{123}I]-VEGF$_{165}$ by planar scintigraphy at 2 h p.i. as described in vivo imaging to obtain a "baseline" uptake. Before taking a second scan, three of the animals were treated with vehicle (PBS) and three were injected intravenously with 80 µg of VEGF$_{165}$. In order to give more evidence for the specific targeting of the VEGFR, one more experiment was performed. Another cell line, CAPAN-II, which is VEGFR-negative, was inoculated in 5 athymic mice. The uptake of the tracer was measured by dissection as described, 2 h p.i.

3. Results and discussion

3.1. Synthesis of [^{123}I]-VEGF$_{165}$ and [^{125}I]-VEGF$_{165}$

The overall radiochemical yield using freshly prepared Iodogen vials is 37% for [^{123}I]-VEGF$_{165}$ and for [^{125}I]-VEGF$_{165}$. A representative chromatogram of the purification step for the ^{123}I compound is shown in Fig. 1. An elution of purified [^{123}I]-VEGF$_{165}$ with PBS/BSA on PD-10 gives rise to a total eluted fraction of 80%. Nonspecific adsorption on the PD-10 column cannot be decreased using increasing amounts of BSA. Radiochemical purity of the ^{123}I tracer recovered at end of synthesis was >95%. Stability of the ^{123}I tracer was >96% for a 4-h incubation period in PBS or DMEM cell growth medium (Table 1). Specific activity for [^{125}I]-VEGF$_{165}$ was 14.2 MBq/mmol. Specific activities of the [^{123}I]-VEGF$_{165}$ tracer were 1.66 10^8 MBq/mmol (3.7 MBq/1 μg injected) for planar scintigraphy, and 3330 or 1665 GBq/mmol for biodistribution studies (74 or 148 kBq/1 μg injected, respectively).

3.2. In vitro assays

Saturation binding plot of [^{125}I]-VEGF$_{165}$ on A2058 cells is shown in Fig. 2. Nonlinear regression reveals K_d=0.11±0.06 nM and B_{max}=9254 ±702 receptors per cell. This is in correlation to the results of Li et al [5], which show a K_d ranging from 0.060 to 0.236 nM. Nonspecific binding was low (NSB coefficient=4.3 X 10^{-4}). The IC_{50} value for displacement of [^{123}I]-VEGF$_{165}$ with native VEGF$_{165}$ was 0.15±0.02 nM. This corresponds to the displacement studies by Li et al., which showed IC_{50} values on various cell lines ranging from 0.009 to 0.245 nM.

Fig. 2: *Saturation binding plot of [^{125}I]-VEGF$_{165}$ on A2058 cells. K_d=0.1±0.05 nM and B_{max}=9453±302 receptors per cell (n =3). Nonspecific binding, specific binding and total binding are represented as curves in the graph.*

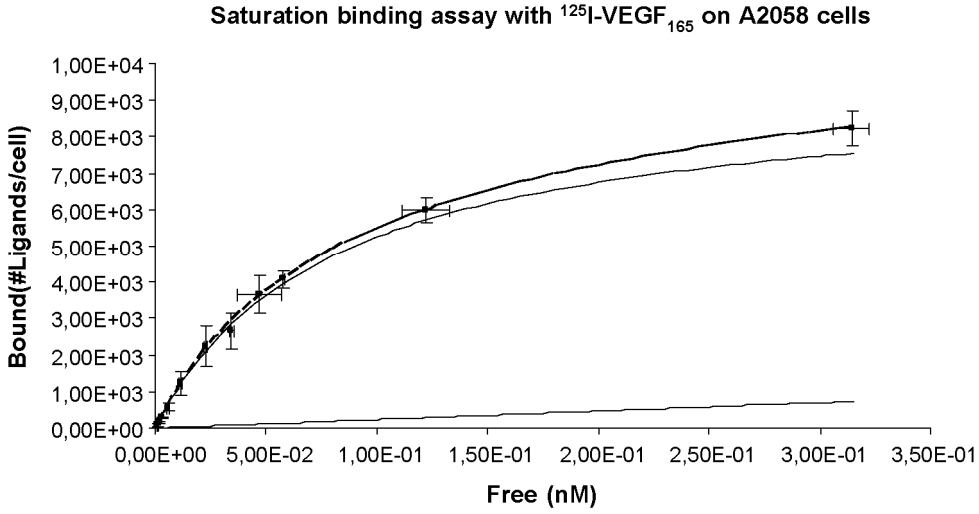

The internalization assay showed uptake of activity in A2058 cells (Fig. 3). The internalized fraction was maximal at 5 h. Afterwards, the curve shows a decrease. The [^{125}I]-VEGF$_{165}$ binds to its receptor and is internalized by ligand-induced endocytosis of the VEGF-VEGFR complex. Afterwards, the vesicle containing the peptide is merged with a lysosome and the tracer is metabolized, resulting in rapid excretion of free $^{123}I^-$ and [^{123}I]-iodotyrosine. Moreover, these results indicate that the ligand-receptor interaction has remained intact after iodination of the VEGF$_{165}$. The possible drawback of the internalization is the metabolization of the tracer and the increased background caused by the secreted products.

3.3. Biodistribution of [^{123}I]-VEGF$_{165}$ and in vivo imaging

Biodistribution of [^{123}I]-VEGF$_{165}$ in NMRI mice showed radioactivity uptake in kidneys (30.1 ± 11.2% ID at 1.5 min), liver (14.6±4.9% ID at 1.5 min) and stomach (13.2±3.5% ID at 3 h). A small uptake was seen in the small and large bowel (Figs. 4A and 5). Low background activity was observed in lungs, heart, body and head (containing the thyroid, which was not dissected separately). When compared to other iodinated peptides, such as [^{123}I]-annexin V [7] or [^{123}I]-hEGF [11], the rather low dehalogenation profile, as observed in the stomach, is

remarkable. Although stomach uptake is still significantly high, it is up to 4 times as low as compared to the other abovementioned radioiodinated peptides. The latter is also confirmed by ROI analysis on both stomach and thyroid on the planar gamma images. Bladder content activity, due to free radioiodine and [^{123}I]-iodotyrosine excretion through the kidneys to the bladder, is found to be high. Background levels in the lungs and intestines are strikingly low, as shown by both biodistribution and planar gamma camera images. These results would make it possible to image tumors, overexpressing the VEGFR-1 or -2 receptors, located in these areas.

Biodistribution in A2058 tumor-bearing athymic mice (Fig. 4B) resulted in a ratio of the %ID/g of the tumor vs. thigh of 0.40±0.14, 6.12±2.11, 1.16±0.30 and 0.48±0.12 at 1, 2, 4 and 6 h p.i., respectively. Other organs did not differ significantly from the results obtained from NMRI mice. The ^{99m}Tc-HSA study shows that the uptake of [^{123}I]-VEGF$_{165}$ in the tumor is not due to increased tumor perfusion: it showed a tumor to muscle ratio of 1.17 (±0.09).

Baseline uptake at 2 h p.i. in A2058-bearing mice resulted in a tumor vs. thigh ratio of 6.01 ±1.95. Vehicle treatment showed no significant difference (ratio= 6.26±1.50; P>>.05). However, co-injection of 80 µg of VEGF$_{165}$ resulted in a significant decrease of the A2058 tumor uptake (ratio = 1.30±0.34; P<.05). These results, added with the in vitro displacement study, suggest the specific uptake of the tracer in the tumor. Ratio tumor vs. thigh of the CAPAN-II-bearing mice was 1.11±0.23.

Because of the absence of labeled catabolites of the tracer, only the native [^{123}I]-VEGF$_{165}$ and free radioiodine are present in plasma. Of these, only the labeled VEGF$_{165}$ can bind to the VEGFR, confirmed by the in vitro displacement experiment.

Fig. 3: *Internalization profile of [^{125}I]-VEGF$_{165}$ in A2058 cells.*

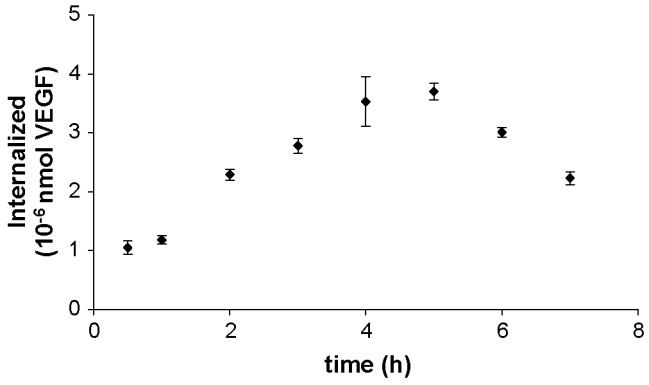

4. Conclusion

Given the preserved receptor-ligand interactions and the high receptor affinity, its low in vivo background activity due to relatively low dehalogenation and good tumor uptake, we conclude that [^{123}I]-VEGF$_{165}$ is a potent tool to perform VEGF receptor scintigraphy in vivo.

Acknowledgment

The authors thank Alexandra Janssens who performed the labeling and stability studies and assisted in the in vitro and in vivo evaluation.

Published in: Nuclear Medicine & Biology (2005), vol.32, iss.5, pp.431-436
Status: Postprint (Author's version)

Fig. 4: *Biodistribution results of [^{123}I]-VEGF$_{165}$ in wild-type NMRI mice (A) and A2058-inoculated nu/nu mice (B).*

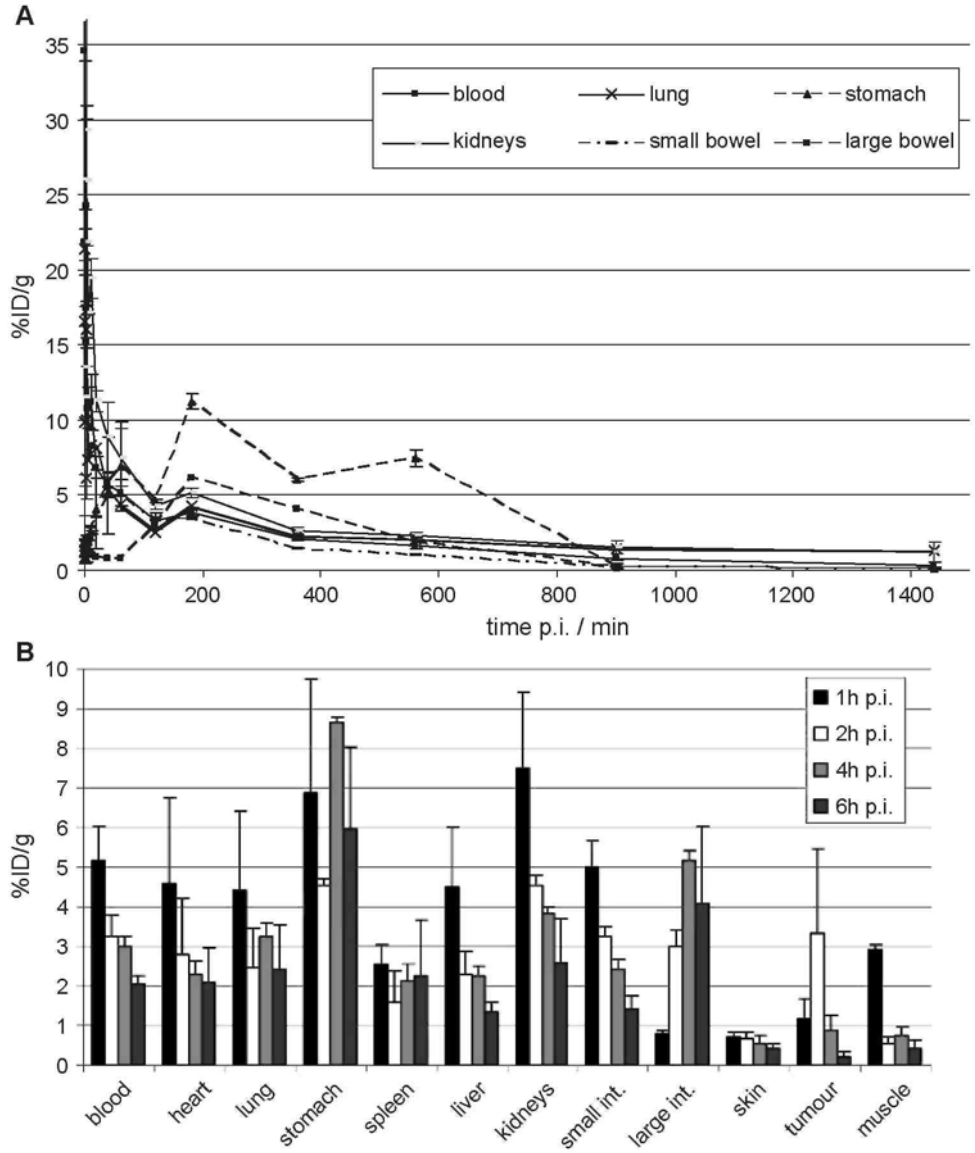

Fig. 5: *Planar gamma camera image of an NMRI mouse (wild type) injected with 3.7 MBq of [^{123}I]-VEGF$_{165}$ at 20 min (left) and 1 h (right) post intravenous injection.*

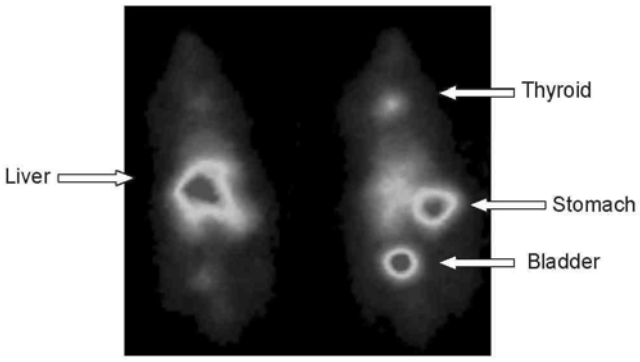

References

[1] Ferrara N, Davis-Smith T. The biology of vascular endothelial growth factor. Endocr Rev 1997;18(l):4-25.

[2] Ferrara N, Gerber H-P, LeCouter J. The biology of VEGF and its receptors. Nat Med 2003;9(6):669-76.

[3] Bhatnagar A, Hustnix R, Alavi A. Nuclear imaging methods for noninvasive drug monitoring. Adv Drug Deliv Rev 2000;41:41-54.

[4] Weissleder R, Mahmood U. Molecular imaging. Radiology 2001;219: 316-33.

[5] Li S, Peck-Radosavljevic M, Koller E, Koller F, Kaserer K, Kreil A, et al. Characterization of ^{123}I-vascular endothelial growth factor-binding sites expressed on human tumour cells: possible implication for tumour scintigraphy. Int J Cancer 2001;91(6):789-96.

[6] Li S, Peck-Radosavljevic M, Kienast O, Preitfellner J, Hamilton G, Kurtaran A, et al. Imaging gastrointestinal tumours using vascular endothelial growth factor-165 ($VEGF_{165}$) receptor scintigraphy. Ann Oncol 2003;14:1274-7.

[7] Lahorte C, Dumont F, Siegers G, Van de Wiele C, Dierckx RA. Synthesis, biodistribution and dosimetry studies of ^{123}I-labelled annexin V in mice: a possible SPET-ligand for visualization of apoptotic cells. Nucl Med Commun 1999;20(10):948-9.

[8] Bylund DB, Yamamura HI. Methods for receptor binding. In: Yamamura, editor. Methods in neurotransmitter receptor analysis. New York (NY): Raven Press; 1990. p. 1-35.

[9] Dumont F, De Vos F, Versijpt J, Janssen HML, Korf J, Dierckx RA, et al. In vivo evaluation in mice and metabolism in blood of human volunteers of [^{123}I] iodo-PK11195: a possible single photon emission tomography tracer for visualizing inflammation. Eur J Nucl Med 1999;26(3):194-200.

[10] Cornelissen B, Jans L, Kersemans V, Oltenfreiter R, Thonissen T, Achten E, et al. Tumour volumetry methods in mice compared with 1 T MRI volumetry. MRI Biomed [submitted for publication].

[11] Cornelissen B, Thonissen T, Kersemans V, Van de Wiele C, Lahorte C, Dierckx RA, et al. Influence of farnesyl transferase inhibitor treatment on epidermal growth factor receptor status. Nucl Med Biol 2004;31:679-89.

[12] Favoni RE, De Cupis A. The role of polypeptide growth factors in human carcinomas: new targets for a novel pharmacological approach. Pharmacol Rev 2000;52(2):179-206.